

# Mixed Synchronous/Asynchronous State Memory for Low Power FSM Design

Cao Cao and Bengt Oelmann

*Department of Information Technology and Media, Mid-Sweden University  
S-851 70 Sundsvall, Sweden  
{cao.cao@mh.se}*

## Abstract

*Finite state machine (FSM) partitioning proves effective for power optimization. In this paper we propose a design model based on mixed synchronous/asynchronous state memory that results in implementations with low power dissipation and low area overhead for partitioned FSMs. The state memory here is composed of the synchronous local state memory and asynchronous global state memory, where the former is used to distinguish the states inside a sub-FSM, and the latter is responsible for controlling sub-FSM communication. The input and output behaviour of the decomposed FSM is cycle by cycle equivalent to the undecomposed synchronous FSM. Together with clock gating technique, substantial power reduction can be demonstrated.*

## 1. Introduction

The majority of low power optimization techniques on architectural level focus on shutting down parts of the circuits that are idle, techniques that go under the name dynamic power management [2]. For the contemporary CMOS technology where the dynamic power dissipation dominates over the static in digital circuits [1], minimizing the switching capacitance is the objective of power minimization. Here, shutting down means preventing idle circuits and nets from switching. Normally, systems are designed to meet a certain peak performance that is only required for a small portion of its entire operational time; therefore, parts of the circuit are often temporarily idle. There are also situations where operations, known in advance, will never be executed at the same time, which always lead to having idle units consequently. In these situations, dynamic power management may be successfully used.

Dynamic power management techniques disable the clock signal or prevent inputs from switching to the parts not in use. In order to do so, mechanism for detecting idle states of different units is needed, also methods for "shut-

ting down" the idle units must be added to the design. Circuits responsible for handling this will constitute a functional overhead and will consequently contribute to increased circuit area, additional power consumption, and possibly reduced speed performance. Careful analysis must be undertaken so that the introduction of circuits for power management will lead to as large power reduction as possible. An optimization procedure for dynamic power management seeks the partitioned system that has the lowest power consumption. The procedure partitions the design after identifying the most beneficial idle conditions taking the overhead of detecting and shutting down circuits into account.

For low power FSM design, the most efficient way is to divide the FSM into two or more sub-FSMs where only one of them is active at a time [3]. The partitioned FSM is constructed in such a way that each of the sub-FSMs will constitute a smaller effective capacitance than the original FSM and consequently power can be saved. Gating the clock signal to shut down the FSM not active is an efficient way and it has been practised in several works, e.g. in [4, 5]. There are two drawbacks in these approaches. First, in minimum length state encoding the area overhead from the increased number of bits in the state memory is substantial for a partitioned FSM. Second, the power consumption for activating and deactivating a sub-FSM is relatively high. These problems have been addressed separately before in e.g. [6] and [7]. In contrast to previous work, we propose a design model that is able to handle both issues in an efficient way.

In the design model for partitioned FSMs we are proposing in this paper, both synchronous and asynchronous state memories are used to implement FSMs with synchronous input/output behaviour. This means that externally the FSM will work as a synchronous FSM but internally there is a mechanism operating asynchronously. This model is the result of our search for finding ways to utilize asynchronous logic in synchronous designs. The general idea is to only use synchronous state memory for state bits that have high probability of changing and asynchronous state memory for those bits with low probability of chang-

ing.

The outline of rest of the paper is as follows. First a presentation is given on approaches to low power FSM design based on FSM partitioning and how the proposed design model is related to them. After that the proposed model is described, first through an example and then by a formal description. This is followed by a description of how to transform a finite state machine specification, in the form of a state transition graph, to the form suitable for implementing it as a partitioned FSM with mixed synchronous/asynchronous state memory. An implementation architecture is then proposed and the effectiveness is illustrated by optimizations through two-way partitioning of a subset of the MCNC FSM benchmarks [8].

## 2. Background

From the point of view of structural decomposition, there are basically two approaches to partition FSMs. The first one is based on separate state memory for each sub-FSM and the second one has shared state memory for all sub-FSMs. The two alternative structures are shown in the figure below. In this section we first introduce the key issues in the implementation of partitioned FSMs, and from that motivate our approach based on mixed synchronous/asynchronous technique.

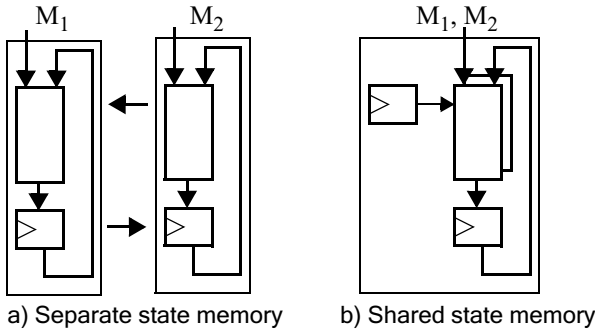


Figure 1. Structural decomposition of FSMs

### 2.1. FSM decomposition with separate state memory

As depicted in Figure 1a) above, each sub-FSM has its own state memory. These state registers are local to the sub-FSM and are referred to as *local state memory*. A state transition with a destination state not residing in the same sub-FSM as the source state we refer to as a *crossing transition*. No global state is needed and the interaction between different sub-FSMs is handled by adding reset states, one in each sub-FSM, to the local states and an additional signal interface for activating and deactivating different sub-FSMs. Assume a *crossing transition* from sub-FSM  $M_1$  to sub-FSM  $M_2$ , when exiting  $M_1$  it turns to its reset state and causes the activation of  $M_2$  that goes

from its reset state to the correct destination state of the *crossing transition*.  $M_1$  will reside in its reset state and shut itself down through gating the clock and input signals.

Power reductions can be achieved through clock gating and disabling the primary inputs to the sub-FSMs not active.

Suppose the original, monolithic machine is partitioned into  $n$  sub-FSMs with the state subsets  $S_1, S_2, \dots, S_n$  respectively, the total number of bits for the local state will be:

$$\sum_{i=1}^n \lceil \log_2 |S_i| \rceil$$

in the case minimum encoding is used. It will always be more bits than what is required in the monolithic implementation. The disadvantage here is the area overhead. The additional flip-flops often constitute a large portion of a state machine. This approach has for example been used in fully synchronous partitioned FSM by Benini et al. [2, 3]. In the events of *crossing transitions* between sub-FSMs there are actually two state transitions taking place (from the source state to the reset state in  $M_1$  and from the reset state to the destination state in  $M_2$ ). This makes *crossing transitions* more power consuming than local transitions. The work by Oelmann et al. [10] introduces a mechanism that makes the *crossing transition* asynchronously and thereby removes the double-clocking requirement, which leads to lower power consumption. This approach leads however to large area overhead mainly due to complex asynchronous logic and large overhead in the output logic.

### 2.2. FSM decomposition with shared state memory

To overcome the problem of the large area overhead, the *local state memory* is shared by all the sub-FSMs [7] as depicted in Figure 1b). Considering the previously described approach, it can be realized that only the state memory in the active sub-FSM is of importance when computing the next state and the outputs, the rest of the state memory is in that sense of no importance. By dividing the states into two parts, global states and local states, the bits for the local states can be shared by all sub-FSMs. The global states decide which one of the sub-FSMs is active. In this way identical state codes can be used for states residing in different sub-FSMs and being distinguished by the global state.

A monolithic FSM is partitioned into  $n$  partitions with state subsets  $S_1, S_2, \dots, S_n$  respectively. The global state needs  $\lceil \log_2 n \rceil$  bits to distinguish between  $n$  sub-FSMs and the local state needs  $\lceil \max(\log_2 |S_1|, \dots, \log_2 |S_n|) \rceil$  bits to represent the sub-FSM with the largest number of states. The total number of bits in the state memory will be lower compared to the separate state memory approach. However, from the power consumption point of view, the disadvantage is that the extra flip-flops for the *global state memory* and the identical number of flip-flops required for each current active sub-FSM. The increased capacitive

load on the clock signal will be the major reason for increased power dissipation.

In the design model for partitioned FSMs introduced in this paper, a shared state memory approach is used where the *global state memory* is asynchronous. The basic idea of having asynchronous *global state memory* comes from the fact that the *crossing transitions*, which lead to changes in the global state, are of low probability and are therefore idle most of the time. By not having the global state continuously clocked, power reduction is achieved. The *local state memory* is kept synchronous and is conditionally clocked based on the number of bits required for the sub-FSM currently active.

### 3. FSM decomposition model

The main objective of this work is to propose a new FSM decomposition model based on mixed synchronous/asynchronous state memory to achieve low power consumption and low circuit overhead. At the same time, the input/output behaviour of the decomposed FSM is identical to the original fully synchronous one.

#### 3.1. Design model overview

In our model, the partitioned sub-FSMs share the same synchronous *local state memory* while asynchronous *global state memory* controls which one of the sub-FSMs should be active. In order to handle *crossing transitions*, the STG is transformed to support an interaction scheme for asynchronously activating and deactivating the sub-FSMs.

After decomposition, the original state set is partitioned into several subsets. State transitions having the source and destination states belonging to the same state subset will be copied without transformation. For every *crossing transition*, an extra *g state* is introduced.

A *crossing transition* is completed by the following sequence of events:

1. A synchronous state transition from the source state of the *crossing transition* to the *g state*, which has the same index as the original destination state.
2. An asynchronous state transition from the *g state* to the original destination state, both of which have the same index.

The first event is called synchronous because the *local state memory* is updated to the *g state* at the active edge of the clock signal. The second event is called asynchronous because it takes place in the *global state memory* upon detection of transitions in the *g states*. The global state is then used to deactivate the currently active sub-FSM, activate the sub-FSM in which the destination state of the crossing transition is. Thanks to the asynchronous global state transition the entire *crossing transition* is completed within one clock cycle.

Consider the STG in Figure 2 and assume a partition of

$M_1$  and  $M_2$ , with state subsets  $S_1 = \{s_1, s_4, s_6\}$  in  $M_1$  and  $S_2 = \{s_2, s_3, s_5, s_7\}$  in  $M_2$ .

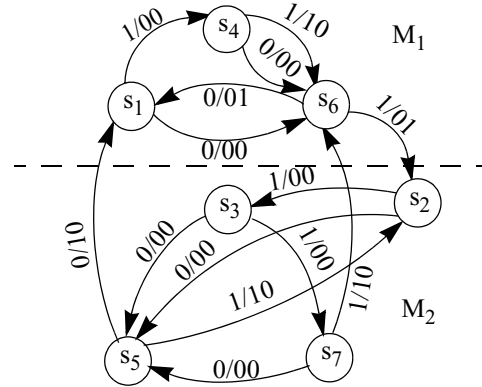


Figure 2. FSM example dk27

Figure 3 shows the transformed STG after decomposition (Input/output is ignored here for clarity). After introducing *g states*, two new state subsets are formed as  $U_1 = \{s_1, s_4, s_6, g_2\}$  in  $M_1$ ,  $U_2 = \{s_2, s_3, s_5, s_7, g_1, g_6\}$  in  $M_2$ .

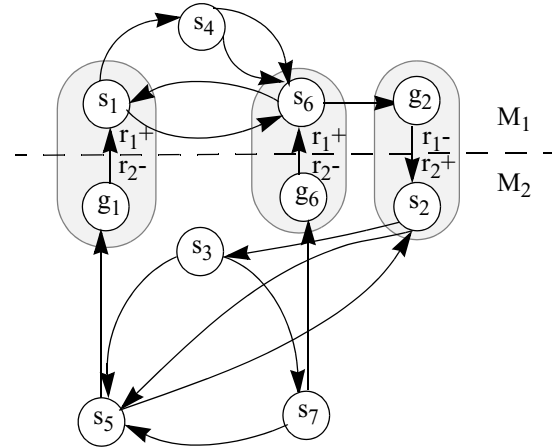


Figure 3. Transformed STG in decomposed FSM

Take the *crossing transition*  $s_6 \rightarrow s_2$  as an example. After  $g_2$  is introduced in  $M_1$ , the first event is the transition  $s_6 \rightarrow g_2$ , inside  $M_1$ . Then at the second event, the detection of  $g_2$  makes the asynchronous state memory update its state from  $r_1$  to  $r_2$  (labelled as  $r_1^-, r_2^+$  on edge  $g_2 \rightarrow s_2$ ). The global states  $r_1, r_2$  indicates the active sub-FSMs  $M_1, M_2$  respectively. After the completion of the asynchronous transition,  $M_1$  is deactivated and  $M_2$  is activated.

The asynchronous transition  $g_2 \rightarrow s_2$  will not influence the *local state memory* which only can be triggered by clock signal; therefore, the source state  $g_2$  and the destination state  $s_2$  will have the same state code, whereas their global states are different. A group of states with identical local state codes and different global states is called a *state*

bundle in this paper. Specially, the *state bundle* including *g state* is called a *g state bundle*. In Figure 3, there are three *g state bundles*  $(g_1, s_1), (g_2, s_2), (g_6, s_6)$  indicated with circles shaded gray.

### 3.2. Definitions

To study state transitions separately, a state machine is defined as a triplet:  $M = (S, I, \delta)$ , where  $S$  is the set of states,  $I$  is the set of binary inputs,  $\delta: S \times I \rightarrow S$  is the transition function.

Let there be a partition on the set  $S$ :  $\pi = \{S_1, \dots, S_n\}$  where  $\pi$  is defined as a collection of  $n$  subsets, called *blocks* also, such that

$$\bigcup_{i=1}^n S_i = S$$

and  $S_i \cap S_j = \emptyset$  for  $i \neq j$  where  $1 \leq i, j \leq n$ .

The monolithic FSM associated with  $S$  is then partitioned into sub-FSMs  $M_1, M_2, \dots, M_n$ .

In state transitions, to reflect the property of states entering or exiting a certain partition *block*  $S_i$ , let us define

$$V(S_i) = \{s_j | \delta(s_j, I) = s_k, s_j \notin S_i, s_k \in S_i\}$$

$$T(S_i) = \{s_j | \delta(s_k, I) = s_j, s_j \notin S_i, s_k \in S_i\}$$

Both  $V(S_i)$  and  $T(S_i)$  are set of states outside block  $S_i$ , the former has state transitions to  $S_i$ ; the latter has state transitions originating from  $S_i$ .

Inside  $S_i$ , let us define:

$$Q(S_i) = \{s_j | \delta(s_k, I) = s_j, s_j \in S_i, s_k \notin S_i\}$$

$$W(S_i) = \{s_j | \delta(s_j, I) = s_k, s_j \in S_i, s_k \notin S_i\}$$

Both  $Q(S_i)$  and  $W(S_i)$  are state subsets inside *block*  $S_i$ , the former has state transitions originating from another partition *block*; the latter has state transitions to another partition *block*.

These four state sets defined above are depicted in Figure 4.

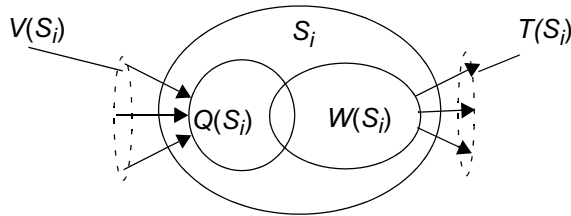


Figure 4. State sets associated with  $S_i$

They will be denoted as  $V_i, T_i, Q_i$  and  $W_i$  in short in the rest of this paper.

### 3.3. Network transformation

According to the definition in section 3.2, the STG transformation is made in the following steps:

#### 3.3.1 Introduce *g states*

For a certain *block*  $S_i$ ,  $G_i$  is a collection of *g states*, which are introduced based on the destination states of *crossing transitions* exiting  $S_i$ .

$$G_i = \{g_k | s_k \in T_i\}$$

The state subset associated with sub-FSM  $M_i$  is then modified from  $S_i$  to  $U_i$ , where

$$U_i = S_i \cup G_i$$

In the transformed network, let us define

$\bigcup_{i=1}^n G_i = G$  as the collection of all *g states* and

$\bigcup_{i=1}^n U_i = U$  as the modified collection of all states. The elements in  $U$  can be generally designated as  $u_k$ , where  $k$  is a subscript variable.

#### 3.3.2 Transition function transformation

The original transition function  $\delta$  is transformed into  $\delta_L$  and  $\delta_G$ , representing the state transition inside the *local state memory* and *global state memory*, separately.

1. Form the local transition function  $\delta_L$ .

Let us define  $\delta_L: S \times I \rightarrow U$  as

$$\delta_L(s_i, I) = \begin{cases} \delta(s_i, I) & \text{if } \delta(s_i, I) = s_k \notin T \\ g_k & \text{if } \delta(s_i, I) = s_k \in T \end{cases}$$

Transitions from a certain set  $W_i$  to  $T_i$  are replaced with transitions from  $W_i$  to the additional introduced set  $G_i$ .

2. Form the global transition function  $\delta_G$ .

The global state set is defined as  $R = \{r_1, r_2, \dots, r_n\}$

There are as many states in  $R$  as the number of sub-FSMs in the partitioned FSM. The global state identical to  $r_i$  indicates sub-FSM  $M_i$  as the active sub-FSM.

Let us define  $\delta_G: R \times U \rightarrow R$  as

$$\delta_G(r_i, u_k) = \begin{cases} r_i^-, r_m^+ & \text{if } u_k \in G_i \\ r_i & \text{otherwise} \end{cases}$$

Where  $r_i^-, r_m^+$  representing the asynchronous state transition. Since  $u_k \in G_i$ , we assume it represents the *g state*  $g_k$ . A *crossing transition* is thus implied and its destination state is  $s_k$ . Thereby,  $r_i^-, r_m^+$  indicates sub-FSM  $M_i$  is deactivated and  $M_m$  satisfying  $s_k \in S_m$  is activated.

### 3.4. State bundling

In section 3.1, we proposed the *g state bundle* and *state bundle* concept through an example. The reasons for state bundling are: 1) It enables states to share the same local state code. 2) It enables an efficient asynchronous hand-over mechanism. 3) The *g state bundle* enables an efficient clock gating implementation.

After the network transformation, a *bundled state table* is built. Every column of the table represents a *state bundle*. A *state bundle* is a set of states with same local state code but different global state code. Every row of the table represents the states in a sub-FSM which have the same global state code. The number of rows is the same as the number of sub-FSMs.

It is known that the *g state* in *G* and its corresponding state in *S* with the same index must be put into the same *g state bundle*, so we build the table beginning with *g state bundles*.

To be specific, let us examine the example in Figure 3 again. Its *bundled state table* is built with two rows, representing  $M_1$  and  $M_2$ , and  $\max(|U_1|, |U_2|)=6$  columns, representing the larger number of states in a single sub-FSM (*g state* is also included). Firstly, three *g state bundles* are put into the table cells shaded gray.

**Table 1. Bundled state table**

B	$b_1$	$b_2$	$b_3$	$b_4$	$b_5$	$b_6$
$M_1$	$s_1$	$s_6$	$g_2$	$s_4$		
$M_2$	$g_1$	$g_6$	$s_2$	$s_3$	$s_5$	$s_7$

Other states in each sub-FSM are then put into the table ordinarily from the leftmost empty cell. We finally get six bundles and every sub-FSM has the same number of bundles as the number of states inside it. After building the *bundled state table*, the state transition inside a sub-FSM can be viewed upon as the *state bundle* transition.

Let us observe the *crossing transition* from  $s_6$  to  $s_2$  again. From Table 1, this transition can be explained in the following sequence: 1) local state transition from *state bundle*  $b_2$  to  $b_3$  inside  $M_1$ . 2) global state transition from  $M_1$  to  $M_2$ , when *local state memory* still resides in  $b_3$ .

### 3.5. State encoding

In the *global state memory*, one hot encoding is used for state encoding. Every global state  $r_i$  is encoded with only one bit to be one and all other bits to be zero. The rest of this section explains how to encode the states in the *local state memory* and the influence of the state assignment to the final gated clock implementation.

State encoding in the *local state memory* has the same meaning as *state bundle* encoding. The requirement on the state bundle encoding is that minimum number of bits in

the state code are changeable for a certain sub-FSM. This will enable efficient clock gating and minimize the size of the combinational logic and often the switching activity of this logic. Binary encoding, which satisfies the requirement, will be used in the rest of the paper. It gives the binary code of zero to the leftmost column of the *bundled state table*. Codes are then increased by one for the columns from left to right.

As mentioned in section 3.4, the number of local state bits is decided by the sub-FSM with the largest number of *state bundles*, that is,  $\lceil \max(\log_2 |U_1|, \dots, \log_2 |U_n|) \rceil$ .

Due to the property of binary encoding, for state transitions inside a sub-FSM  $M_i$ , only  $\lceil \log_2 |U_i| \rceil$  bits can be changed. These bits are called the *changeable bit field* of  $M_i$ . Other bits which are always zero can be called *don't care bits* of  $M_i$ . Thereby, when  $M_i$  is active, only the *changeable bit field* needs to be triggered by the clock signal and taken as inputs to the combinational logic of  $M_i$ . One thing that needs to be pointed out is each *changeable bit field* related with a certain sub-FSM is decided by the global state; therefore, it only changes after the global state asynchronous transition, that is, the next clock cycle after the *crossing transition*. The problem left is how we can get the correct code in *local state memory* when there is a *crossing transition* between two sub-FSMs with different *changeable bit fields*. This problem is solved by the introduction of *g state bundles* which give extra restrictions to the state encoding. The *g state* which is in the same sub-FSM as the source state of the *crossing transition*, working as a transition state, makes the source and destination state of a *crossing transition* have their local state codes within the same *changeable bit field* of the current active sub-FSM. Accordingly, the current sub-FSM's *don't care bits* which keep zero after the completion of the *crossing transition* will not influence the correct code of the *crossing transition* destination state.

To be specific, we examine the example in Figure 3 again and binary encoding is assigned in the *bundled state table*.

From Table 2, we can see the number of local state bits is three. In  $M_1$ , only bit0 and bit1 are changeable and belong to the *changeable bit field*. The bit2 which is always zero is regarded as *don't care bit* of  $M_1$ . In  $M_2$ , all three state bits are in its *changeable bit field*.

**Table 2. State encoding for bundled state table**

B	$b_1$	$b_2$	$b_3$	$b_4$	$b_5$	$b_6$	$\lceil \log_2  U_i  \rceil$
	000	001	010	011	100	101	
$M_1$	$s_1$	$s_6$	$g_2$	$s_4$			2
$M_2$	$g_1$	$g_6$	$s_2$	$s_3$	$s_5$	$s_7$	3

Suppose there is a *crossing transition* from  $s_5$  in  $M_2$  to  $s_1$  in  $M_1$ . After the synchronous transition from  $b_5$  to  $b_1$ , the *local state memory* is changed to "000". Bit2 becomes zero and will be disabled in the next clock cycle after the

asynchronous transition from  $M_2$  to  $M_1$ . If there is a *crossing transition* from  $s_6$  in  $M_1$  to  $s_2$  in  $M_2$  reversely, after the synchronous transition from  $b_2$  to  $b_3$ , the local state memory will be changed to “010”. The  $g$  state bundle  $b_3$  makes the highest bit of  $s_2$  zero only, which is restricted by  $g_2$ . Without this encoding restriction, a *crossing transition* from  $M_1$  to  $M_2$  may require the local code to change from “001” to “110”, for example, then the disabled bit2 is still zero and the result will be “010” instead. In other words,  $g$  state bundles ensure a correct state code in the *local state memory* after the completion of the *crossing transition*.

## 4. Implementation structure

In this section we first propose a general structure for our decomposed FSM model. Then we give a detailed description of the implementation. For clarity we limit ourselves to describing the two-way partitioned FSM.

### 4.1. N-way partitioning structure

Suppose the monolithic machine has  $I$  as input,  $O$  as output and is partitioned into sub-FSMs  $M_1, M_2, \dots, M_n$ . The original state subsets  $S_1, S_2, \dots, S_n$ , combining the introduced  $g$  states, form the new state subsets  $U_1, U_2, \dots, U_n$  for  $M_1, M_2, \dots, M_n$ , respectively. All sub-FSMs share the same *local state memory* but have their own combinational logic. Our decomposed FSM structural model is shown in Figure 5.

The  $G$  state bundle Detection Logic (referred to as GDL) decodes the state bits in the *Local State Memory* (referred to as LSM). If a  $g$  state bundle is detected, a signal is sent to the *Global State Memory* (referred to as GSM).

GSM decides the current active sub-FSM. It is implemented as an asynchronous finite state machine. A state transition in the GSM only takes place at the event of a *crossing transition*, that is, when a  $g$  state has been detected. In a “well-partitioned” FSM, where the probability of a *crossing transition* is low, the GSM will be idle most of the time and will therefore dissipate no dynamic power. The state information in the GSM is directly used as control signals to both the LSM and the combinational part (implementing the next state and primary output function) of the sub-FSMs (labeled  $M_1 \dots, M_n$  in Figure 5).

As pointed out in section 3.5, the number of local state bits to the combinational part of  $M_i$  is  $\lceil \log_2 |U_i| \rceil$ . For an active  $M_i$ , only the *changeable bit field* of the LSM is clocked when the other bits are disabled by clock gating. The global state controls the clock gating.

At any given time, except for the events of *crossing transitions*, only one sub-FSM is active. The active sub-FSM is responsible for determining the primary output and the next local state. When inactive, all its inputs are disabled by AND gates and no dynamic power will be dissipated. All outputs of an inactive sub-FSM are set to zero. By using OR gates, the correct primary outputs and next

state outputs can be obtained by collecting corresponding outputs from all sub-FSMs.

It is known that the number of state bits into the combinational logic of a sub-FSM is important to its implementation size and is also related to the power dissipation. This partitioning of a FSM results in a less number of state bits needed for sub-FSMs. Reduction in both area and power can thus be achieved. Large power reductions is obtained when a good partitioning is found where a small sub-FSM active most of the time.

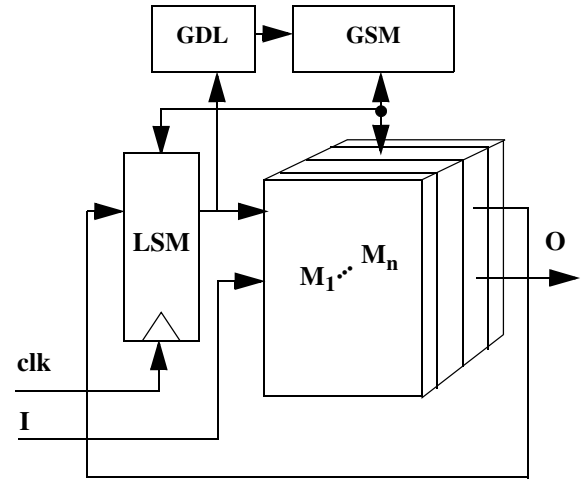


Figure 5. Structural model based on mixed synchronous/asynchronous state memory

### 4.2. Two-way partitioning implementation

For the sake of clarity, we limit ourselves to present the detailed implementation architecture for two-way partitioning, but it can easily be extended to FSMs with more partitions. In addition, according to our experiments, two-way partitioning can result in large power savings.

To be specific, we examine the example in Figure 2 again. The original STG is transformed in Figure 3 and *bundled state table* is set up in Table 1. Local state codes are given in Table 2. The global state set is defined as  $R=\{r_1, r_2\}$  and the state codes of  $r_1$  or  $r_2$  are indicated as  $(n_1, n_0)$ , where  $(n_1, n_0)=01$  represents that sub-FSM  $M_1$  is active,  $(n_1, n_0)=10$  represents that sub-FSM  $M_2$  is active. By one-hot encoding of the global state, it is possible to decode the active sub-FSM directly from the state bits.

Figure 6 shows the block diagram for the overall realization. The  $G$  state bundle Detection Logic (GDL) detects the local states. The  $g$  state bundle  $b_1, b_2$ , and  $b_3$  (in Table 1) corresponds to the output signal  $a$  ( $a_0a_2$ ), which are sent to the *Global State Memory* (GSM).

The clock gating logic for glitch-free operation is com-

posed of a NAND gate and an inverter here. Three bits are needed for the local state since  $M_2$  has six states, but only two bits are needed for  $M_1$ . The bundled state encoding restriction results in that the lower two bits FF1, FF0 in the *Local State Memory* (LSM) are always active and are therefore directly controlled by the global clock. State bit FF2 is not used in  $M_1$  and is therefore conditionally clocked. The global state bit  $n_1$  controls the clock gating of FF2. The highest bit FF2 is always zero when  $M_1$  is active, in which case it is disabled. When  $M_2$  is active the global state bit  $n_1$  equals one and enable the clock signal of FF2.

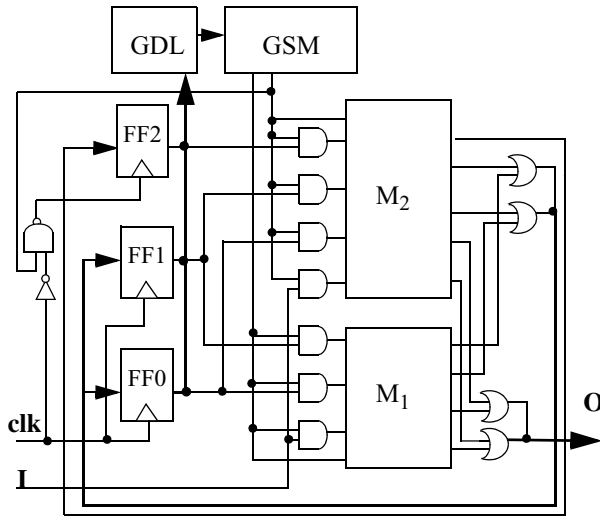


Figure 6. Circuit of a decomposed FSM(dk27)

Besides clock gating, disabling of the inputs to the combinational logic is used to reduce the power dissipation. In our example, the input disabling logic is implemented by three AND gates in front of  $M_1$  and four AND gates in front of  $M_2$ . Depending on the global bits, these AND gates can block the state bits and primary input signals from propagating through  $M_1$  or  $M_2$ .

Both the primary outputs and the next state values are computed by both sub-FSMs but separated in time. The signals from  $M_1$  and  $M_2$  have to be merged. There are four OR gates. Two of them are used to decide the correct primary output; the other two are used for FF0 and FF1. Note that FF2 is *don't care bit* to the combinational part of  $M_1$  and it is only updated by the next state signal from the combinational part of  $M_2$ .

For two-way partitioning, it is shown by Figure 7 that GSM is composed of two asynchronous memory elements AS0 and AS1 with output  $n_1$ ,  $n_0$  respectively. AS0 is reset by AS1 and set by the signal which is a collection of  $g$  state in sub-FSM  $M_2$  (see  $g_1$  and  $g_6$  in Table 1). AS1 is reset by AS0 and set by a collection of  $g$  state in sub-FSM  $M_1$  (see  $g_2$  in Table 1).

Suppose there is a *crossing transition* from  $s_6$  in  $M_1$  to  $s_2$  in  $M_2$ . At the beginning, global state bits  $(n_1, n_0)=01$ . In the first step, the *local state memory* is updated by the  $g$  state bundle  $b_3$ . In the second step, after detecting  $b_3$ , GDL will set the output  $a_2$  to be one and send this signal to GSM. In GSM, together with its own feedback signal  $n_0=1$ ,  $g_2$  is detected, which set AS1 immediately. AS1 will then reset AS0. Now  $(n_1, n_0)=10$  and the *crossing transition* from  $M_1$  to  $M_2$  is completed. The completion of  $g_2$  signal can be depicted by the signal sequence:  $g_2^+$ ,  $n_1^+$ ,

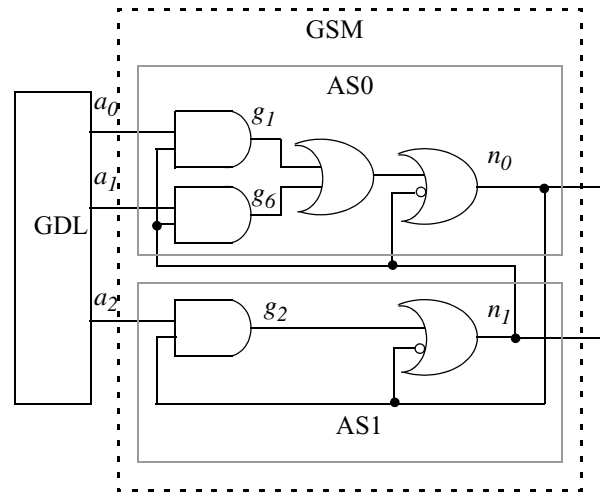


Figure 7. Global state memory structure in dk27

$n_0^-$ ,  $g_2^-$ , where “+” represents a monotonical change from 0 to 1, “-” represents a monotonical change from 1 to 0.

Through this example, the whole procedure for two-way FSM decomposition is explained, also the potential is shown that a good partition with unbalanced size of sub-FSMs can efficiently reduce the area size in the combinational logic. The structure inside asynchronous *global state memory* (in Figure 7) is similar for all two-way partitioning and used in the experiments of the next section.

## 5. Experimental results

By two-way decomposition, our solution of mixed synchronous/asynchronous state memory was applied on circuits from the standard benchmark set. The number of states in the benchmarks range from 19 to 121 states.

For state partitioning, we use Kernighan-Lin algorithm to find a small cluster of states composing the first sub-FSM and all other states composing the second one [9]. The cost function is based on transition probability and the smaller sub-FSM should has high probability of state transitions inside itself, and low probability of *crossing transitions* to the other sub-FSM.

The power dissipation was obtained from gate level power estimation by Power Compiler (Synopsys), assuming a supply voltage of 1.8V, a clock frequency of 20MHz.

The area estimation was based on the cell area and the target technology is a 0.25 $\mu$ m CMOS standard cell technology.

The primary input probability was set to 0.5 and its switching activity was set to 0.5 also. The stationary state probabilities are computed based on random-walk simulations.

In Table 3, characteristics of the original finite state machine are shown. The circuit name, input, output and number of states are given in the first four columns. The area and power statistics is given in the last two columns.

**Table 3. Finite state machine statistics**

Circuit	#PI	#PO	#states	area	power
s1488	8	19	48	924.7	155.9
s820	18	19	25	443.9	71.1
s1494	8	19	48	899.5	136.7
styr	9	10	30	427.9	54.3
keyb	7	2	19	271.2	68.0
s832	18	19	25	466.5	75.9
scf	27	56	121	786.1	76.3

\* power:  $\mu$ W area: #gate eq

**Table 4. Results after decomposition**

Circuit	$ S_1 / S_2 $	$ U_1 / U_2 $	area	power	%A	%P
s1488	4/44	6/48	821.7	51.4	-11.1%	67.0%
s820	5/20	7/23	505.5	40.2	+13.9%	43.5%
s1494	4/44	6/48	841.0	50.5	-6.5%	63.1%
styr	4/26	6/29	534.8	43.0	+25.0%	20.8%
keyb	4/15	7/16	330.9	39.9	+22.0%	41.3%
s832	3/22	4/24	506.5	39.7	+8.6%	47.7%
scf	6/112	8/114	963.7	46.8	+14.3%	38.7%

\* power:  $\mu$ W area: #gate eq

In Table 4, The column labeled “ $|S_1|/|S_2|$ ” shows the state subsets for respective partition in the decomposed FSM. The column labeled “ $|U_1|/|U_2|$ ” shows the modified state subsets after introducing  $g$  states. The following two columns show the area, power of the decomposed FSM. The percentage area increase, power reductions of the decomposed FSMs are shown in the last two columns. An average power reduction of 46.0% is achieved with an area increase of 9.5%. For benchmarks such as *s1488*, power reduction can be up to 70%.

## 6. Conclusions

In this paper we propose a novel design model for partitioned FSMs that is based on mixed synchronous/asynchronous state memory. In spite of the internal

asynchronous operation, the input/output behaviour of the decomposed FSM is equivalent to the synchronous one. By applying this model to a number of standard FSM benchmark circuits using two-way partitioning, we have demonstrated that large power reductions (up to 70%) can be achieved with low or no area overhead.

The partitioning and STG transformations are made automatically in our prototype tool, which takes an STG as input, generates synthesizable RT-level VHDL code that is fed to a standard logic synthesis tool. A standard CMOS cell-library can be used without the need of any special cells.

In this work we have not paid any special attention to the optimization of state clustering and state encoding. We believe that there is room for further power reductions when these issues are addressed.

We also believe the mixed synchronous/asynchronous state memory concept deserves further investigation. By applying it to  $n$ -way partitioning, more power reductions can be expected, especially for large FSMs.

## 7. REFERENCE

- [1] 1999 ITRS Roadmap.
- [2] L. Benini and G. De Micheli, “Dynamic Power Management - Design Techniques and CAD Tools,” *Kluwer Academic Publisher*, 1998.
- [3] L. Benini and G. De Micheli, “Automatic Synthesis of Low-Power Gated Clock Finite-State Machines,” *IEEE Transactions on Computer-Aided Design for Integrated Circuits and Systems*, 1996, vol. 15, no. 6, pp. 630-643.
- [4] L. Benini, P. Siegel, and G. De Micheli, “Saving Power by Synthesizing Gated Clocks for Sequential Circuits,” *IEEE Design and Test of Computers*, 1994, vol. 11, pp. 32-41.
- [5] E. Hwang, F. Vahid, and Y-C. Hsu, “FSMD Functional Partitioning for Low Power,” in *Proceedings of Design and Test in Europe*, March, 1999, pp. 22-28.
- [6] B. Oelmann and M. O’Nils, “Asynchronous Control of Low-Power Gated Clock Finite-State Machines,” in *Proceedings of the IEEE International Conference on Electronics, Circuits, and Systems*, 1999, pp. 915-918.
- [7] S-H. Chow, Y-C. Ho, and T.Hwang, “Low-Power Realization of Finite-State Machines - A Decomposition Approach,” *ACM Transactions on Design Automation of Electronics Systems*, 1996, vol. 1, no. 3, pp. 315-340.
- [8] Yang. S, (1991) Logic Synthesis and Optimization Benchmarks User Guide, version 3.0, MCNC Technical Report.
- [9] J.Monteiro, A.Oliveira “Finite State Machine Decomposition for Low Power,” in 35th Design Automation Conference, June, 1998, pp. 758-763.
- [10] B. Oelmann, M. K. Tammemäe, M. Kruus, and M. O’Nils, “Automatic FSM Synthesis for Low-Power Mixed Synchronous/Asynchronous Implementation,” *Journal of VLSI Design 2001, Special Issue on Low-Power Design*, vol. 12, no. 2, pp. 167-186.